VIII International Conference on Computational Methods in Marine Engineering
MARINE 2019
R. Bensow and J. Ringsberg (Eds)

EXPERIMENTAL AND NUMERICAL INVESTIGATION OF BLADE GEOMETRY EFFECT ON PROPELLER CAVITATION AND NOISE

MARINE 2019

XIAO-QIAN DONG*, QI WANG, CHEN-JUN YANG

State Key Laboratory of Ocean Engineering(SKLOE)
Collaborative Innovation Center for Advanced Ship and Deep-Sea Exploration(CISSE)
Shanghai Jiao Tong University, Shanghai 200240, China
*e-mail: xiaoqiandong0330@sjtu.edu.cn

Key words: Propeller, Blade geometry, section profile, skew, tip rake, Cavitation, Noise

ABSTRACT: In this paper, the effects of propeller blade geometry on cavitation and noise were studied by model tests and numerical simulations. Section thickness distribution, skew and tip rake are considered. Propeller model tests were carried out in SJTU Cavitation Tunnel. Test results of open water performance, cavitation inception and noise were compared. Then the hydrodynamic performances were simulated by solving the Reynolds-averaged Navier-Stokes (RANS) equations using the Fluent software. The boundary layer grids were set on blades. Numerical results of open water performance, section pressure distribution and propeller wake flow field were compared. It is shown that increasing skew can delay cavitation inception, and reduce the area of sheet and sound pressure level after cavitation occurs; increasing skew near blade tip can delay tip vortex cavitation inception further at low advance coefficients; thickening the section near leading edge can delay the suction side and pressure side cavitation inception, and make cavitation stable when cavitation incepts; tip rake can reduce the strength of tip vortex, and delay the tip vortex cavitation inception significantly.

1 INTRODUCTION

With Modern ships developing towards larger size and higher speed, cavitation and noise performances of propeller are increasingly important. One of the key objectives of propeller optimization is to delay propeller cavitation inception and reduce propeller noise. When propeller blades rotate, there is pressure differences between the upstream and downstream surfaces, which drives the secondary flow around the blade tip, and leads to the tip vortex. The low pressure at the core of the tip vortex will cause cavitation, and the tip vortex cavitation is generally earlier than the sheet cavitation. Once cavitation occurs, the noise of propeller will increase significantly, sometimes even cause the vibration on ship stern.

In propeller design, tip unloading (reducing pitch and camber of tip), is usually used to delay the tip vortex cavitation inception, but tip unloading has a negative impact on propulsion efficiency [1] [2]. On the other hand, some researchers began to study how to delay the tip vortex cavitation inception by changing skew and rake near the tip. Kuiper [3] studied the effects of skew and rake on cavitation inception, and the results show that tip rake towards pressure side can delay the tip vortex cavitation inception. Choi [4] also studied the effects of skew and rake

on the cavitation and fluctuating pressure. Yamasaki [5] compared the effects of tip unloading and tip rake on the hydrodynamics, cavitation and fluctuating pressure through experimental study. It was found that tip rake is better than tip unloading in reducing the area of cavitation and fluctuating pressure. Subsequently, Yamasaki [6] made further research on the influence of tip rake on the fluctuating pressure, the size and distribution of tip rake were studied experimentally, and the relationship between the reduction of the fluctuating pressure and tip rake was regressed according to the experimental data. Xin [7] studied the effects of tip thickness, skew and rake on tip vortex flow and cavitation inception with three-dimensional twisted hydrofoil. Using geometry with rake towards pressure side can prevent the leading edge vortex rolling into the local tip vortex and weaken the transverse flow around tip.

In this paper, the effects of propeller blade geometry, section thickness distribution, skew and tip rake, on cavitation and noise were studied by model tests and numerical simulations. Propeller model tests were carried out in SJTU Cavitation Tunnel. Also the hydrodynamic performances were simulated by solving the Reynolds-averaged Navier-Stokes (RANS) equations using the Fluent software. Test results of open water performance, cavitation inception and noise were compared. The boundary layer grids were set on blades. Numerical results of open water performance, section pressure distribution and propeller wake flow field were compared.

2 EXPERIMENTAL RESEARCH

2.1 Test facility and measuring equipments

Propeller model tests were carried out in the cavitation tunnel of Shanghai Jiao Tong University (SJTU CT), as shown in Figure 1. The test section is 6.1m in length, and its cross section is 1m×1m with rounded corners. The axial flow velocity over the test section ranges from 0.5m/s to 15.8m/s, and the static pressure at the centerline of the test section ranges from 25kPa to 300kPa. The non-uniformity of axial flow velocity is less than 1%.

Figure 2 shows the equipments used in the model tests. The measuring ranges of the single propeller dynamometer are ±3000N for thrust and ±300Nm for torque, respectively. The maximum rotating speed is 1750r/min. The propeller model was mounted upstream the dynamometer. Propeller noise was measured by Brüel & Kjær 8103 hydrophone, which was just below the propeller model, with a distance of 0.725m, fixed in the acoustic measurement tank. The frequency response range of the hydrophone is 0.1Hz ~ 180Hz, and the sensitivity is -211dB re 1V / μPa ± 2dB.

Figure 1: The cavitation tunnel of Shanghai Jiao Tong University

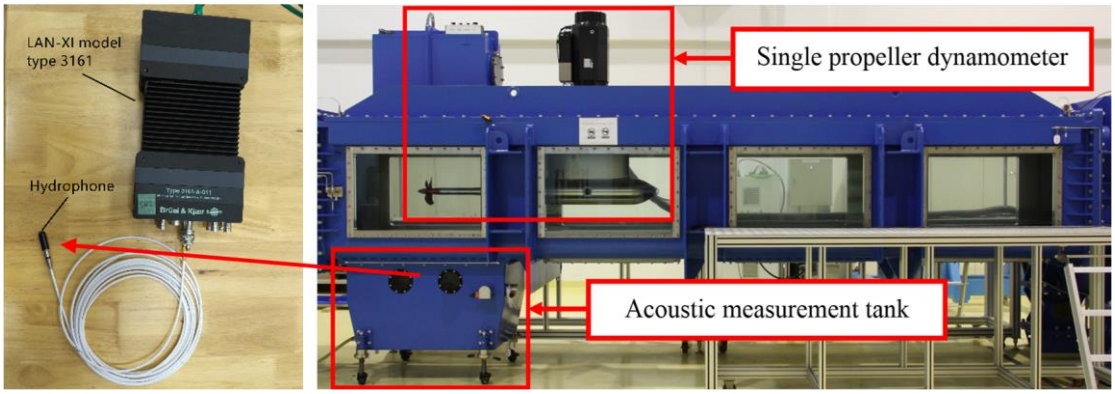

Figure 2: The equipments used in propeller model tests

2.2 Propeller models

Five propeller models with different skew, tip rake and section thickness distribution are used for model tests. The model diameter D is 250mm. DTMB 4381 propeller [8] was used as the initial model, which is a five-blade propeller without skew. DTMB 4382 propeller, a five-blade propeller with a linear skew of 36°, was used to study effect of skew angle. (Pitch and camber of 4382 propeller are correct due to skew, the pitch distributions are shown in Figure 1.) Based on the 4382 propeller, another three propellers were designed. For the 4382-1 propeller, the maximum thickness of section profile is unchanged, but the thickness near leading and trialing edges is increased, as shown in Figure 4. Comparing with 4382-1 propeller, a balance skew distribution is used on 4382-2 propeller, as shown in Figure 5. Comparing with 4382-2 propeller, a tip rake of 2%D towards pressure side is used on 4382-3 propeller, as shown in Figure 6. The pitch (Figure 1), camber and chord for these three propellers are same with 4382 propeller. Figure 7 shows the comparison of blade profiles, while Figure 8 give a 3D viewer of the tip rake. Figure 9 shows the photos of five propeller models.

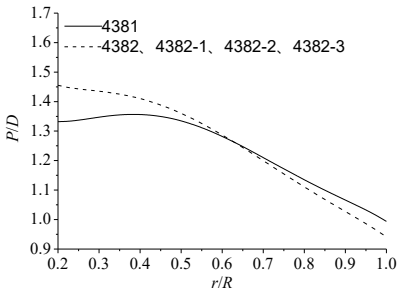

Figure 3: Pitch distribution

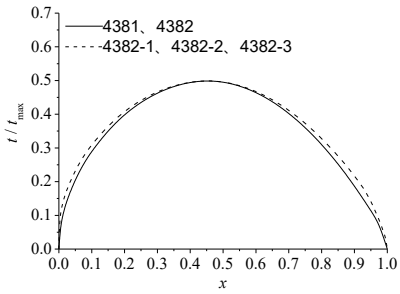

Figure 4: Section profile

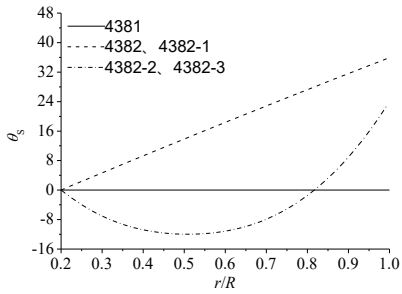

Figure 5: Skew distribution

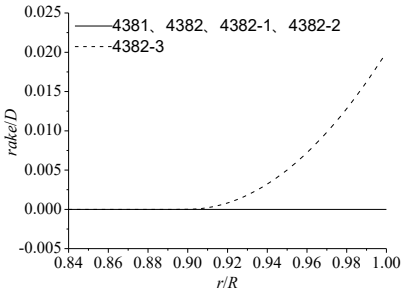

Figure 6: Tip rake

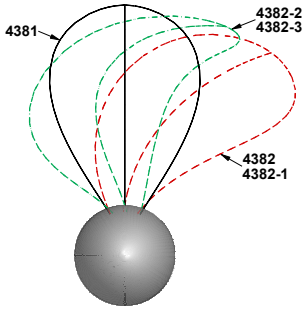

Figure 7: Blade outline

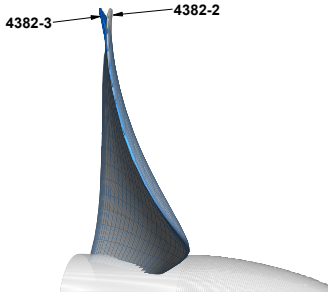

Figure 8: 3D view of tip rake

4381 4382 4382-1 4382-2 4382-3

Figure 9: Photos of propeller models

2.3 Test results and analysis

- Open Water Performance

The open water test was carried out with a constant rotating speed of 20r/s. The Reynolds number ranges from 7.5×10^5 to 8.7×10^5, which is defined as

$$Re = \frac{C_{0.7R}\sqrt{V_A^2 + (0.7\pi nD)^2}}{v} \tag{1}$$

where $C_{0.7R}$ is the chord length at $0.7R$, V_A is the advance velocity, n is propeller rotating speed and v is the kinematic viscosity of water.

Figure 10 shows the comparison of SJTU CT test results and DTNSRDC test results [8]. For the SJTU CT test results, thrust and torque are larger at most J conditions. One possible reason is that the test results in SJTU CT is not corrected with blockage effect of cavitation tunnel and dynamometer.

Figure 11 compares the open water performance of five propellers, and K_T, K_Q and η_0 at design condition J=0.889 are presented in table 1. The performances of five propellers are close at most J conditions, the relative differences of K_T, K_Q and η_0 between each propeller are within 3.9%, 4.5% and 1.2%, respectively, at design condition J=0.889 It can be approximately considered that performances of the five propellers are the same under design condition.

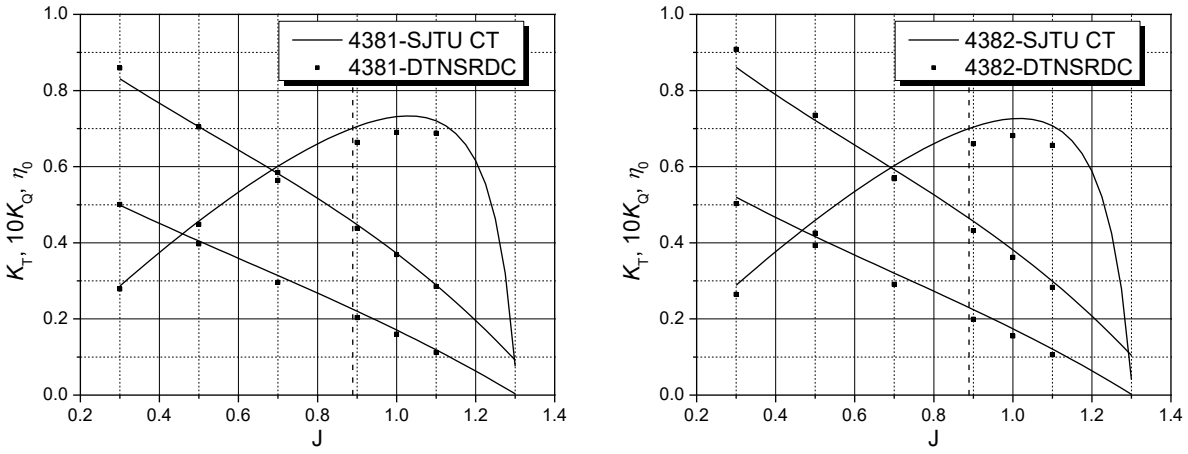

Figure 10 Comparison of open water performance test results with DTNSRDC (Left: 4381 propeller, Right: 4382 propeller)

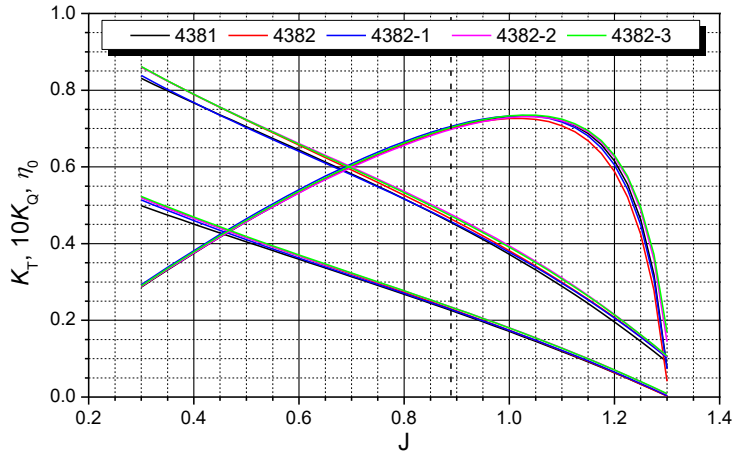

Figure 11: Comparison of open water performance of the five propellers

Table 1: The open water performance at design condition (J=0.889)

	4381	4382	4382-1	4382-2	4382-3
K_T	0.226	0.230	0.228	0.235	0.235
$10K_Q$	0.455	0.464	0.457	0.476	0.473
η_0	0.701	0.700	0.706	0.698	0.703

- Cavitation Inception

The cavitation inception test was carried out with a constant rotating speed of 20r/s. At each advance coefficient J, the cavitation test was conducted by starting from a noncavitating condition and reducing the cavitation tunnel pressure until one kind of cavitation appeared. The cavitation number is defined as

$$\sigma_n = \frac{P_0 - P_v}{\frac{1}{2}\rho n^2 D^2} \tag{2}$$

where P_0 is the static pressure at the propeller shaft, P_v is the vapor pressure of water, and ρ is the density of water. Figure 12 shows the comparison of cavitation inception curves of the five propellers.

Compared with 4381 propeller, the cavity bucket of 4382 propeller (with a linear skew of 36°) became much wider. Both of the suction side and pressure side cavitation inceptions were delayed a lot. Also the tip vortex cavitation inception was delayed, which is more obvious at low advance coefficients.

Compared with 4382 propeller, the suction side and pressure side cavitation inceptions of 4382-1 propeller (with a section profile thickened near leading and trailing edges) were delayed slightly. The tip vortex inception was only delayed near design condition. And during cavitation test, it was seen that inception of sheet cavitation on 4381 and 4382 propeller was highly unstable, the inception pressure in each decompression cannot repeat well, which was much better on 4382-1 propeller.

Compared with 4382-1 propeller, using a balanced skew distribution made the cavitation inception of 4382-2 propeller delay further. Delay of tip vortex inception was very obvious at low advance coefficients, which was similar to the delay of tip vortex cavitation between 4381 and 4382 propeller. Using the balanced skew distribution corresponds to increasing the skew at outer radius.

Compared with 4382-2 propeller, by using tip rake (towards pressure side), the tip vortex cavitation inception of 4382-3 propeller was delayed significantly. On the suction side, the cavitation inception was delayed at low advance coefficients; while tip rake had little effect on the pressure side cavitation inception.

In summary, increasing skew can delay tip vortex cavitation, suction side cavitation and pressure side cavitation inception significantly, and increasing skew near blade tip can delay tip vortex cavitation inception further at low advance coefficients; thickening the section profile near leading edge can delay the suction side and pressure side cavitation inception, and make cavitation stable when cavitation incepts; tip rake can delay the tip vortex cavitation inception significantly.

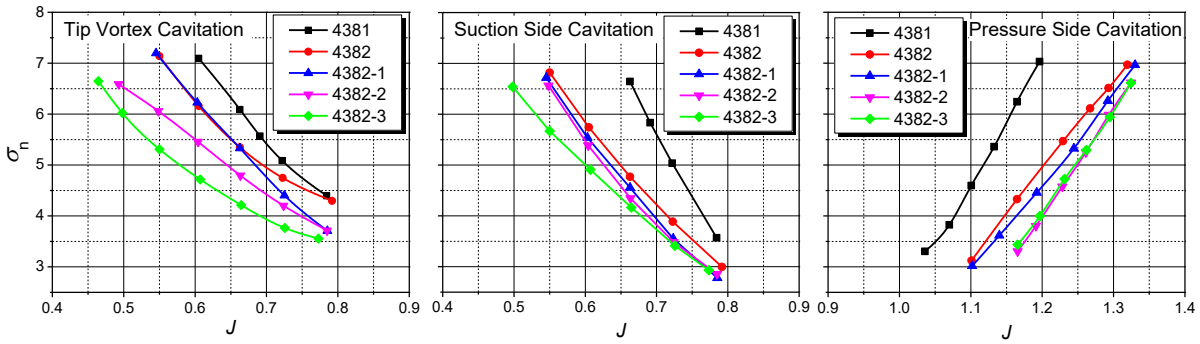

Figure 12: Cavitation inception test results

- Noise

Propeller noise measurements were conducted under J=0.5 and σ_n=5.73. The background noise was also measured under the same condition.

Figure 13 shows the cavity patterns on the five propellers under the noise test condition. Sheet cavitation was seen on 4381, 4382, 4382-1 propeller, and the cavitation area decreased along radial and chordwise directions one by one. Stable and strong tip vortex cavitation was observed on these three propeller. Cavitation on 4382-2 and 4382-3 propeller were much weaker, both of the sheet and tip vortex cavitation appears intermittently, and the tip vortex cavitation on 4382-3 propeller was weaker due to the tip rake.

Figure 14 shows the sound pressure level of five propellers. Increasing skew can decrease the sound pressure level, at high frequency, larger than 10kHz, based on comparison of 4381 and 4382 propeller, as well as 4382-1 and 4382-2 propeller. At low frequency, between 300Hz to 2000Hz, two peaks appeared in the noise spectrum of 4381 propeller, at about 600Hz and 1000Hz; noise spectrum of 4382 had the same shape but lower peak value; from 4382-1 propeller to 4382-3 propeller, noise spectrum at low frequency became smooth one by one, and the maximum sound pressure level decreased correspondingly.

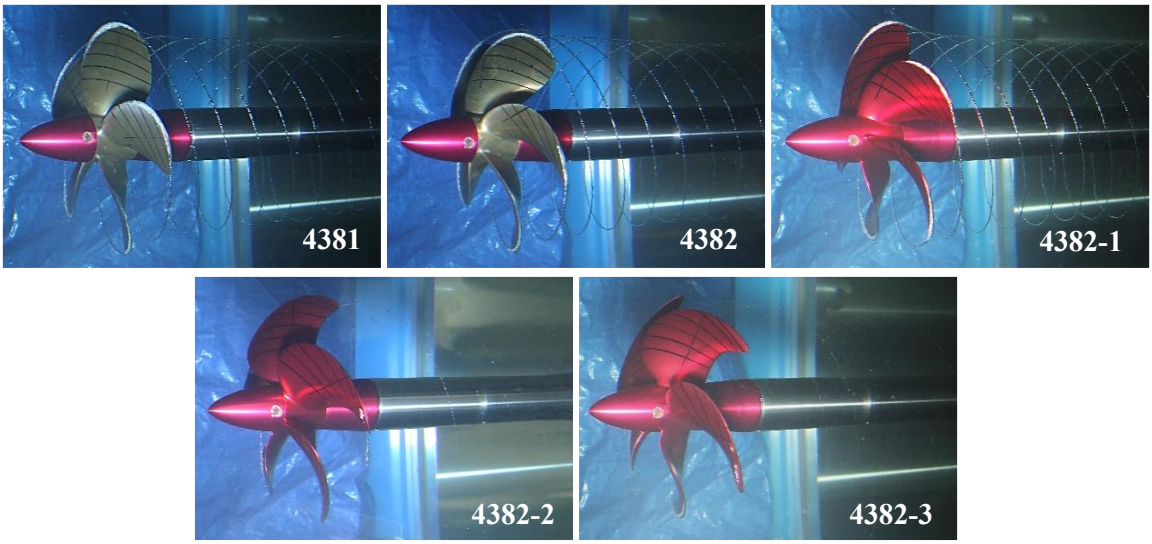

Figure 13: Comparison of cavity patterns of five propellers (J=0.5, σ_n=5.73)

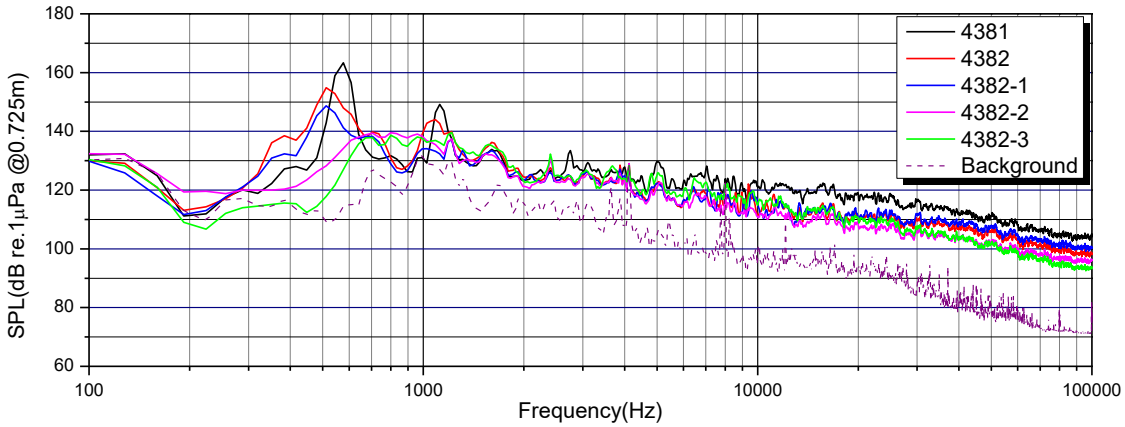

Figure 14: Comparison of sound pressure level of five propellers (J=0.5, σ_n=5.73)

3 NUMERICAL SIMULATION

3.1 Modeling

Since flow in open water is assumed to be steady and periodic for all blades in the coordinate system fixed to the propeller, a single blade passage suffices for the simulation. As illustrated in Figure 15, the computational domain is a portion of the cylinder which is coaxial with the propeller shaft. It is bounded by a pair of periodic surfaces which pass through the shaft axis and make an angle of 360/*Z* degrees, where *Z* is the number of blades, and here *Z*=5. The inlet and outlet of the domain are 5*D* upstream and 10*D* downstream of the propeller. The radial size of the domain is 5*D*. As shown in Figure 16, the periodic boundary surfaces pass through the leading and trailing edges of adjacent blades, hence the back and face of the adjacent blades, instead of the same blade, become boundaries of the domain. By doing so, prism layer grids of high quality can be generated easily on blade surfaces, as shown in Figure 17. Using the SST k-ω model for turbulence closure, the boundary layer flow is resolved down to the viscous sub-layer. The wall distance averaged over blade surfaces, y+, and total number of cells are presented in table 2. All the boundary surfaces are discretized via triangular grids, while the space outside the prism layers is discretized via tetrahedral cells.

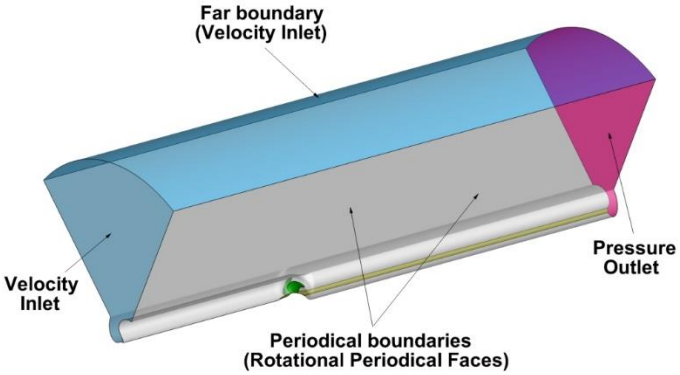

Figure 15: The computational domain

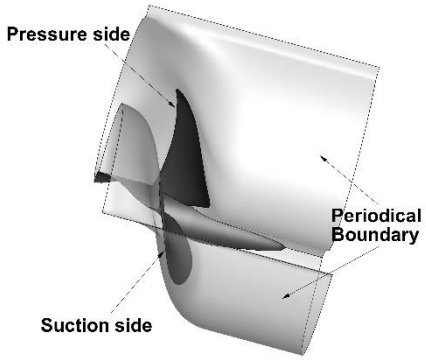

Figure 16: Geometry of the sub-domain enclosing the back and face of adjacent blades

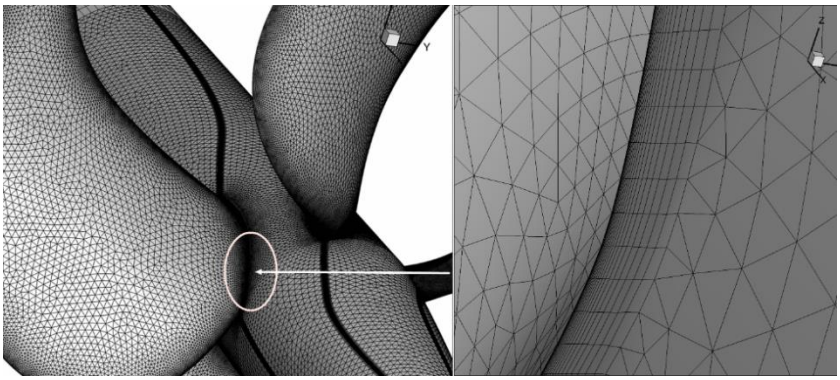

Figure 17: Zoom-up view of blade-surface prism layer grids

Table 2: Wall distance averaged over blade surfaces (y+) and total cells number

	4381	4382	4382-1	4382-2	4382-3
y+	1.41	1.47	1.19	1.16	1.38
Total cells number (million)	5.31	5.40	5.45	6.57	5.93

The blade, hub, and shaft surfaces are set as stationary no-slip walls in the rotating frame. As shown in Figure 15, the inlet and far boundary are set as velocity inlets, while the outlet as the pressure outlet. For a fixed rotation speed of the propeller, the inlet velocity is specified according to the desired value of J, the advance coefficient.The convection terms in all the governing equations are discretized with 2nd-order upwind schemes. The SIMPLE scheme is employed for velocity-pressure coupling.

3.2 Numerical results and analysis

Figure 18 compares the numerical results of the open water performance for five propellers, and K_T, K_Q and η_0 at design condition J=0.889 are presented in table 3. The numerical results that the performances of five propellers are close except low advance coefficient, the relative differences of K_T, K_Q and η_0 between each propeller are within 3.0%, 3.3% and 1.3% at design condition, respectively.

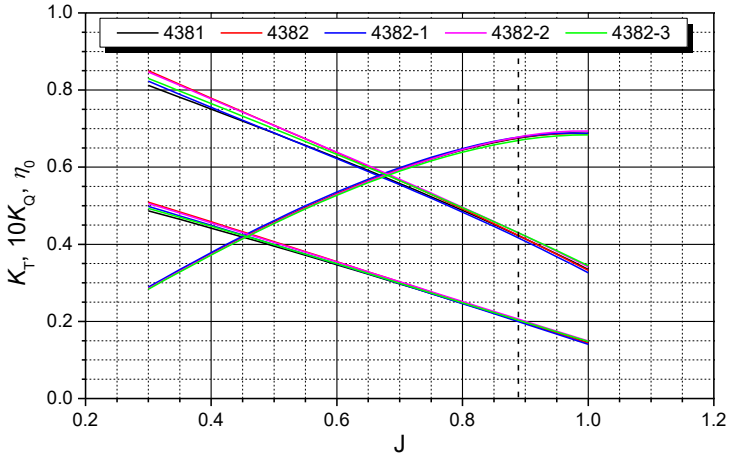

Figure 18: Numerical results of open water performance of the five propellers

Table 3: Numerical results of open water performance at design condition (J=0.889)

	4381	4382	4382-1	4382-2	4382-3
K_T	0.202	0.202	0.200	0.206	0.203
$10K_Q$	0.422	0.423	0.416	0.429	0.430
η_0	0.675	0.677	0.678	0.678	0.669

Figure 19 and 20 shows the section pressure coefficient distribution along the chord of 0.75R and 0.97R at J=0.7 and J=0.889. The horizontal axis is dimensionless chordwise coordinate x/C, and x/C=0 at leading edge, x/C=1 at trailing edge. The peak of negative pressure near leading edge decreases from 4381 propeller to 4382-2 propeller at 0.75R under J=0.7 and J=0.889,

which agrees with the cavitation test that the radial range of sheet cavitation decreases from 4381 propeller to 4382-2 propeller. And for 4382-3 propeller, the tip rake affects little at 0.75R. Comparing 4382-2 and 4382-3 propeller, the load on tip is reduced due to the tip rake. At 0.97R, comparing 4382-1 and 4382-2 propeller, increasing skew at outer radius reduces the pressure difference between the suction and pressure side near the leading edge at J=0.7, which can explain the reason of tip vortex inception delay with balance skew distribution at low advance coefficients.

Figure 19 and 20 shows the pressure coefficient contour of the plane perpendicular to the shaft axis, 0.1D downstream from the blade tip, at J=0.7 and J=0.889. It is seen that the strength of tip vortex decreases in turn from 4381 propeller to 4382-3 propeller, which coincides with the test results of tip vortex cavitation inception.

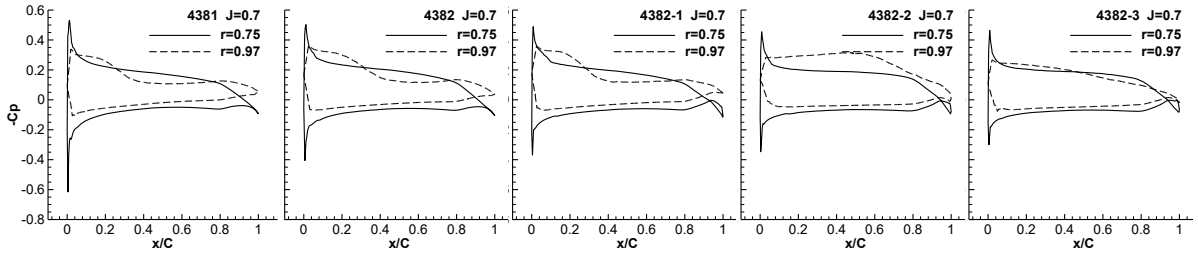

Figure 19: Section pressure at 0.75R and 0.97R (J=0.7)

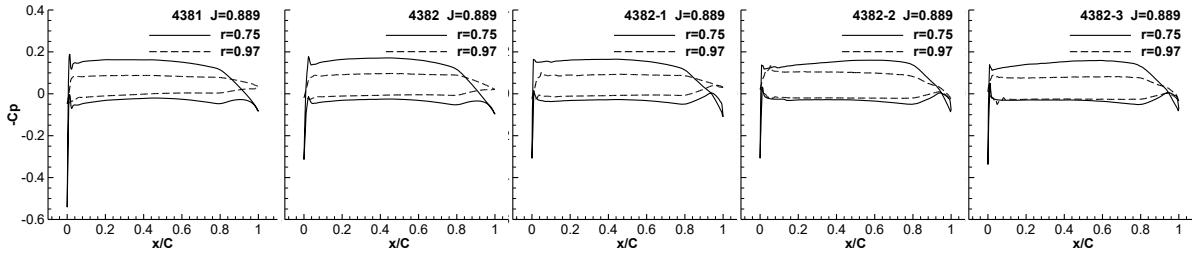

Figure 20: Section pressure at 0.75R and 0.97R (J=0.889)

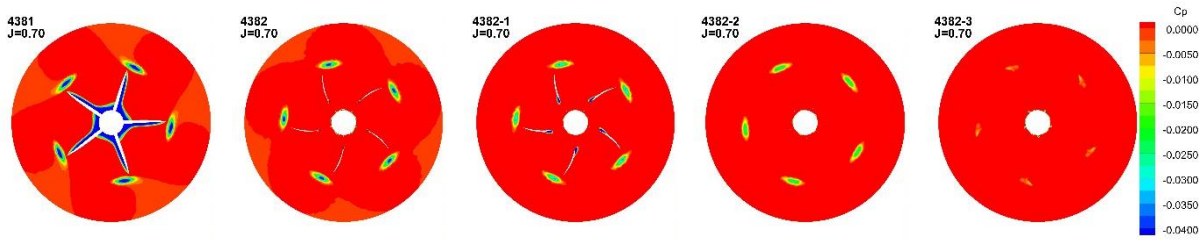

Figure 21: Pressure fields in the cross section 0.1D downstream of the tip (J=0.7)

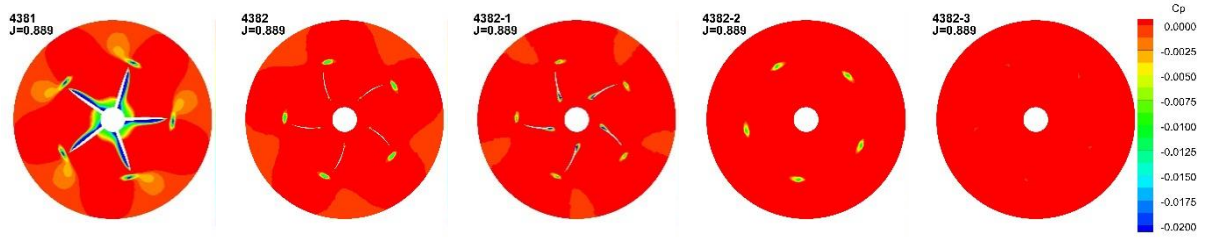

Figure 22: Pressure fields in the cross section 0.1*D* downstream of the tip (*J*=0.889)

4 CONCLUSIONS

In this paper, the effects of propeller blade geometry, section thickness distribution, skew and tip rake, on cavitation and noise were studied by model tests and numerical simulations. Propeller model tests were carried out in SJTU Cavitation Tunnel. Also the hydrodynamic performances were simulated by solving the Reynolds-averaged Navier-Stokes (RANS) equations using the Fluent software. According to the test and numerical results, the following conclusions are drawn,

- Increasing skew can delay tip vortex cavitation, suction side cavitation and pressure side cavitation inception significantly. Increasing skew near blade tip can delay tip vortex cavitation inception further at low advance coefficients. After the cavitation occurs, increasing skew can reduce the area of the sheet cavitation, and decrease the sound pressure level at high frequency.
- Thickening the section profile near leading edge can delay the suction side and pressure side cavitation inception, and make cavitation stable when cavitation incepts.
- Both of skew and section thickening at leading edge can decrease the peak of negative pressure near leading edge.
- Tip rake can reduce the strength of tip vortex, and delay the tip vortex cavitation inception significantly.

REFERENCES

[1] Chiba N., A relation between circulation distribution and tip vortex cavitation of marine propellers [C]. AIAA, 27th Joint Propulsion Conference, Sacramento, CA, USA, June 24-26, 1991.

[2] Stainer M.J., The effect of radial circulation distribution on propeller cavitation [C]. PROPCAV ’95 Conference on Propeller Cavitation, Newcastle upon Tyne, UK, 1995.

[3] Kuiper G., Effects of skew and rake on cavitation inception for propellers with thick blade sections [C]. 20th Symposium on Naval Hydrodynamics, Santa Barbara, USA, 1994.

[4] Choi G.I., The effect of propeller skew and rake on the fluctuating pressure [J]. Journal of the Korean Society of Marine Engineering, 21(4), 1997, pp364-371.

[5] Yamasaki S., Okazaki A., Design and model tests of a backward tip rake propeller for a low speed ship [J]. The Japan Society of Naval Architects and Ocean Engineers, Vol.5, 2007, pp163-168.

[6] Yamasaki S., Okazaki A., et al., The effect of tip rake on propeller induced pressure fluctuations [J]. The Japan Society of Naval Architects and Ocean Engineers, Vol.17, 2013,

pp9-17.
[7] Xin G.Z., The Investigation of the effect of blade geometry on tip vortex cavitation inception and its mechanism[D], China Ship Research & Development Academy, March 2014.
[8] Boswell R.J., Design, cavitation performance, and open-water performance of a series of research skewed propellers [R]. Report No.3339, America: Naval Ship Research and Development Center, 1971.